

Ethylamine-Driven Amination of Organic Particles: Mechanistic Insights via Key Intermediates Identification

Peiqi Liu¹, Jigang Gao¹, Yulong Hu¹, Wenhao Yuan², Zhongyue Zhou², Fei Qi², and Meirong Zeng¹

¹College of Smart Energy, Shanghai Jiao Tong University, Shanghai 200240, P.R. China

²School of Mechanical Engineering, Shanghai Jiao Tong University, Shanghai 200240, P.R. China

Correspondence to: Meirong Zeng (meirongzeng@sjtu.edu.cn)

Summary of this file:

The number of pages: 14

The number of sections: 2

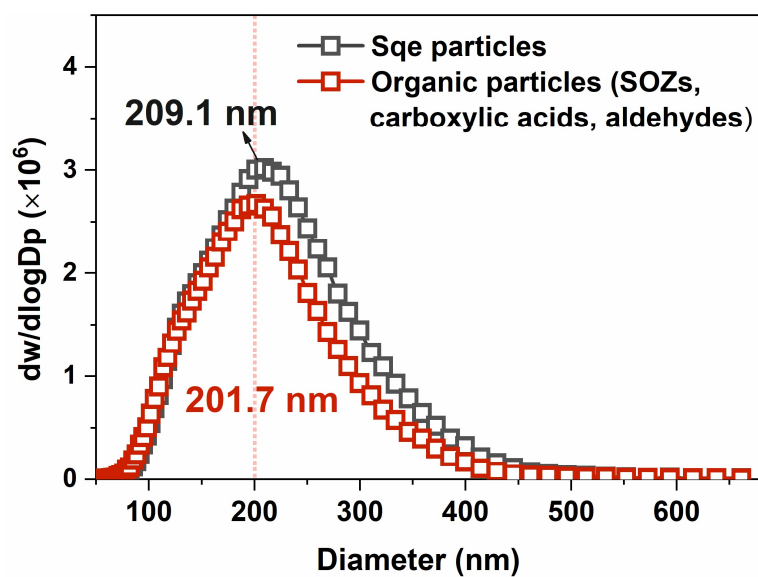
- Section S1. Supporting experimental data

- Section S2. Reaction mechanisms

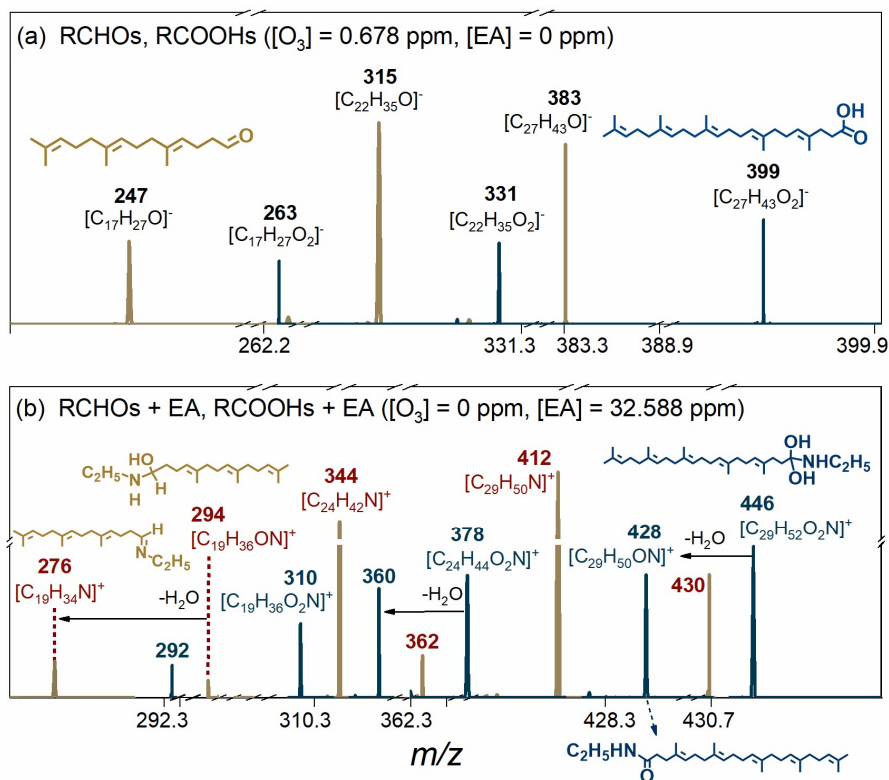
The number of figures: 14

16 Section S1. Supporting experimental data

17 This section presents supporting experimental data consisting of particle size distributions (Fig. S1), reaction products
18 distributions (Figs. S2 and S3), kinetic profiles (Fig. S4), APPI-HRMS (Fig. S5), and uptake coefficients (Figs. S6 and S7).



19
20 **Figure S1.** Size distributions of Sqe particles and organic particles measured by SMPS. The diameters of organic particles (201.7 nm) is
21 comparable to that of Sqe particles (209.1 nm).



22

23 **Figure S2.** Mass spectra of (a) representative aldehydes (RCHOs) and carboxylic acids (RCOOHs) generated from Sqe ozonolysis in the
 24 first flowtube reactor, and (b) their amination products upon ethylamine (EA) exposure in the secondary flowtube reactor.

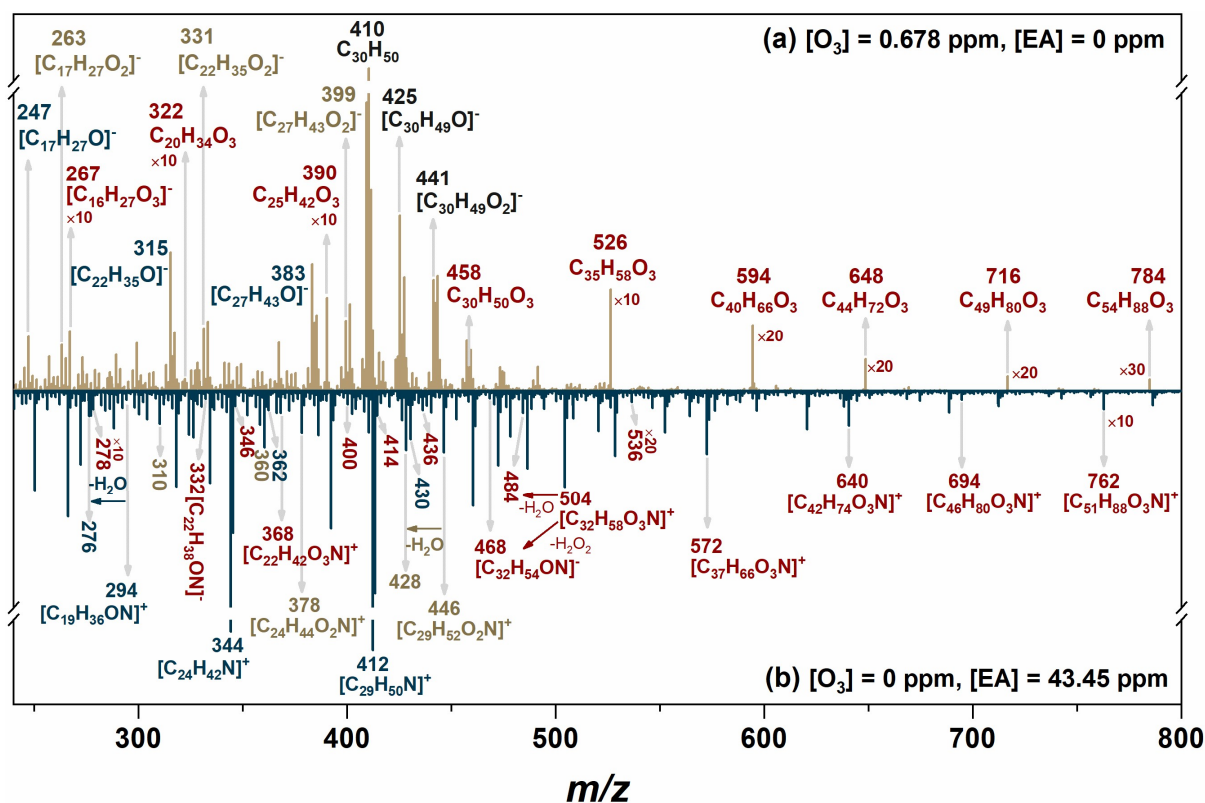


Figure S3. Products distributions from (a) Sqc ozonolysis at 0.678 ppm O_3 in the first flowtube reactor, and (b) subsequent amination reactions with ethylamine ($[EA] = 43.45$ ppm) in the secondary flowtube reactor.

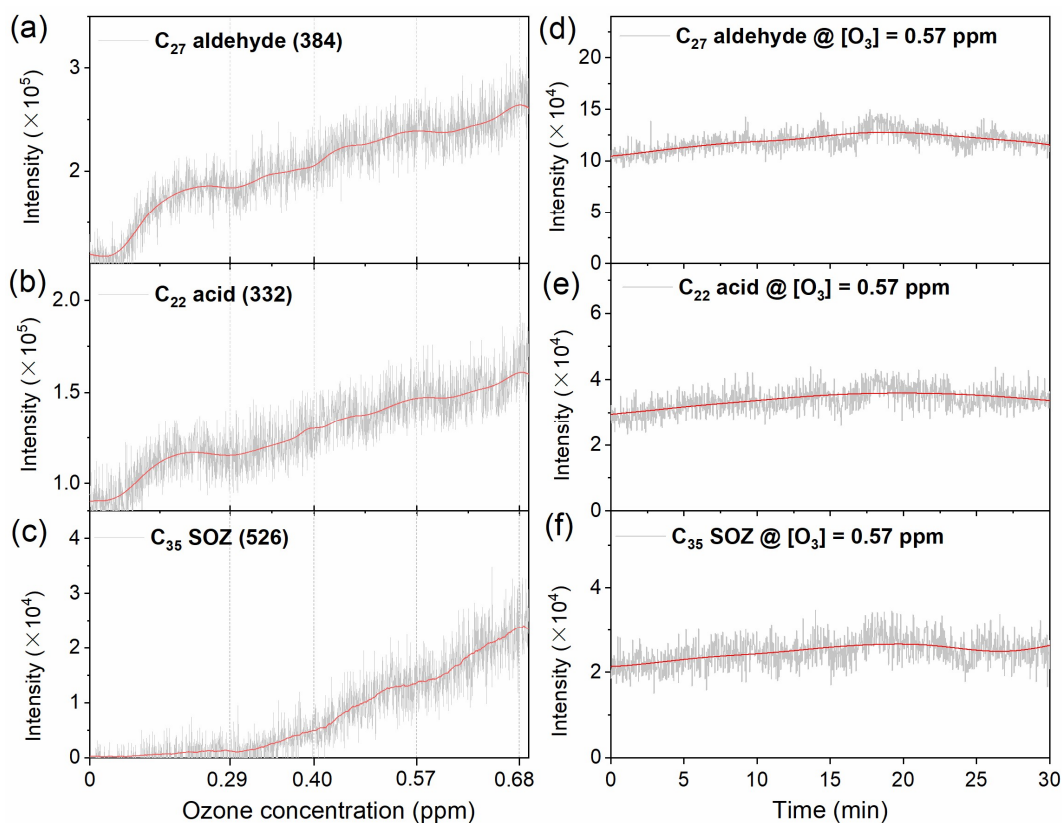


Figure S4. Mass spectral intensities of representative C_{27} aldehyde (MW 384), C_{22} carboxylic acid (MW 332), and C_{35} SOZ (MW 526) in the first flowtube reactor under (a-c) varying O_3 concentrations (0, 0.29, 0.4, 0.57, and 0.68 ppm); as well as (d-f) at fixed O_3 concentration (0.57 ppm).

Figure S5 shows the direct orifice-sampling interface coupled with particle evaporation and photoionization for APPI-HRMS analysis (Liu et al., 2024). The particles flow (800 mL/min) was introduced into the online detection system through a quartz glass tube (235 mm long \times 8 mm i.d.), featuring a 0.5 mm sampling orifice. Particles are vaporized by a heater positioned outside the tube (maintained at 180 $^{\circ}C$) ensure particle vaporization prior to ionization. A vacuum ultraviolet (VUV) lamp (PKS106, Heraeus, Ltd.) with a photon energy of 10.6 eV (117 nm) provides soft photoionization, minimizing fragmentations during ionization.

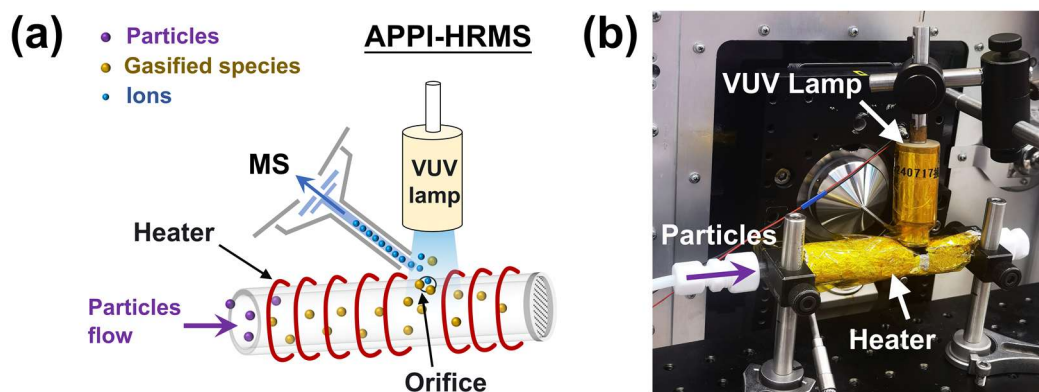


Figure S5. (a) Schematic diagram and (b) photograph of the direct-orifice sampling interface integrated with online APPI-HRMS.(Liu et al., 2024)

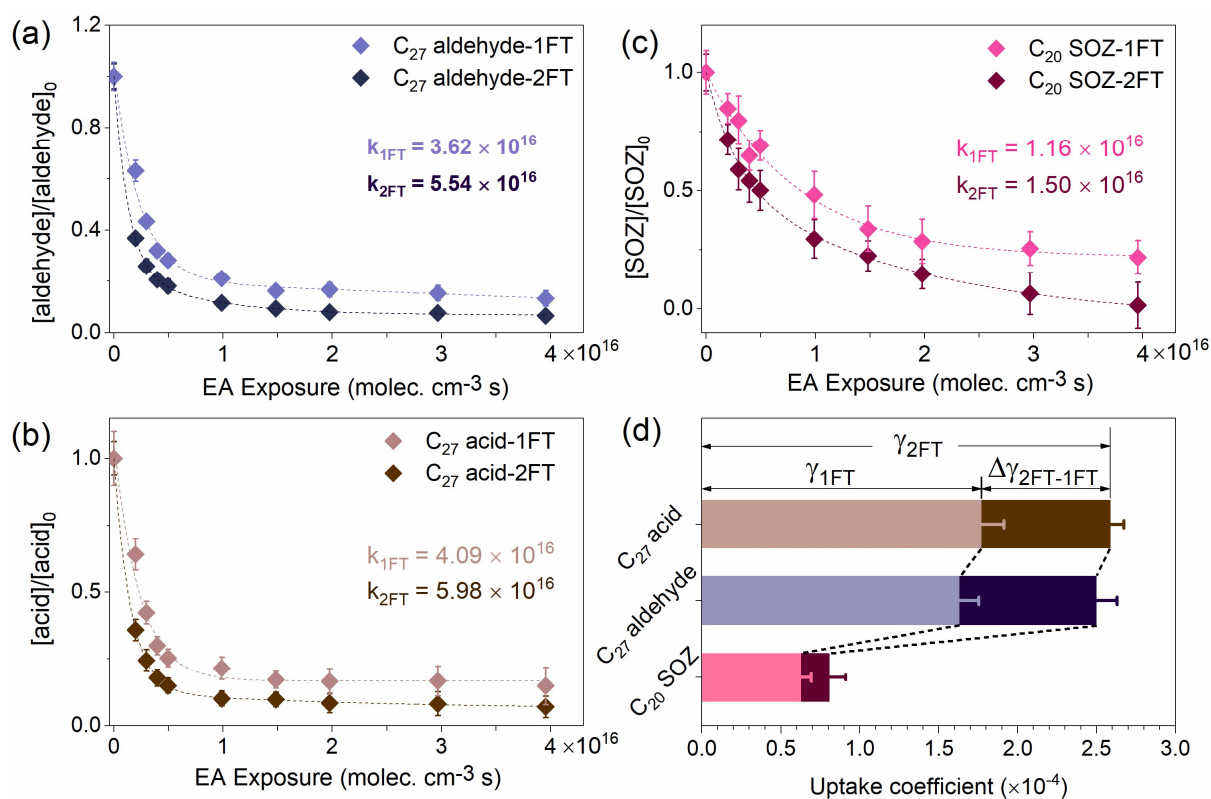
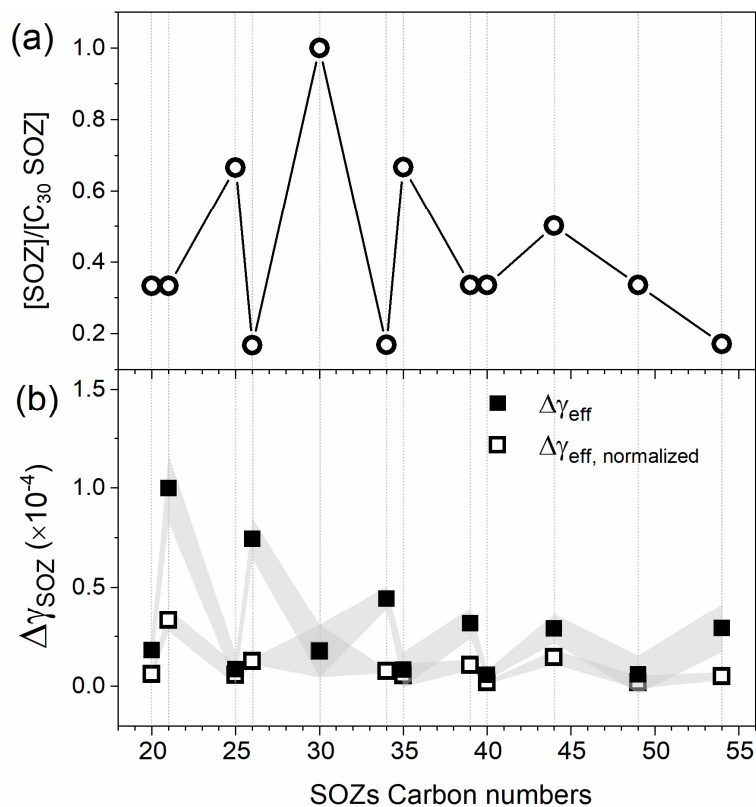


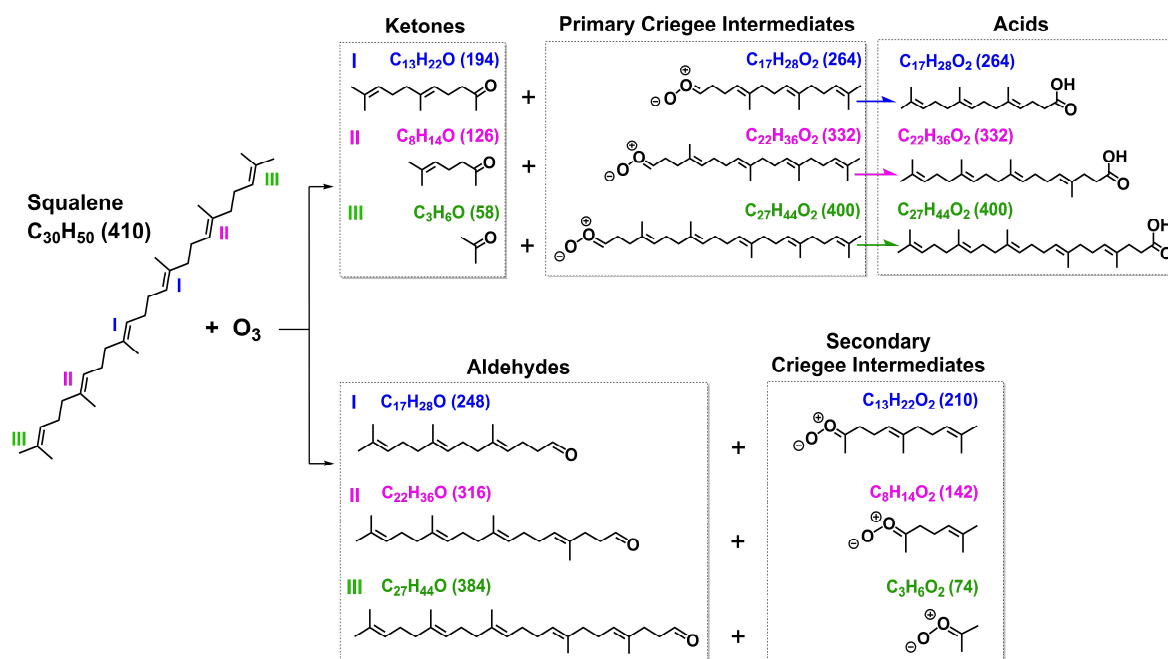
Figure S6. (a-c) The decay kinetics of representative (a) C_{27} aldehyde, (b) C_{27} carboxylic acid, and (c) C_{20} SOZ under control single flowtube experiment (1FT) and tandem flowtube reactor experiment (2FT). The derived decay rates of these organic particles (denoted as k_{1FT} and k_{2FT}) were used to calculate (d) the differential uptake coefficients ($\Delta\gamma_{2FT-1FT}$), revealing the net reaction contribution in the secondary flowtube reactor.



46
 47 **Figure S7.** (a) Relative abundances of SOZs normalized to the C₃₀ SOZ (maximum concentration) based on data from Ref.(Liu et al., 2024;
 48 Heine et al., 2017). (b) Experimentally determined differential uptake coefficients (denoted as $\Delta\gamma_{\text{eff}}$) for C₂₀ to C₅₄ SOZs were normalized
 49 by their relative abundances of yield $\Delta\gamma_{\text{eff, normalized}}$. The reduced differences in $\Delta\gamma_{\text{eff, normalized}}$ values exhibit compared to original $\Delta\gamma_{\text{eff}}$ values
 50 demonstrates that the abundance of SOZs influence their heterogeneous reactivity with ethylamine.

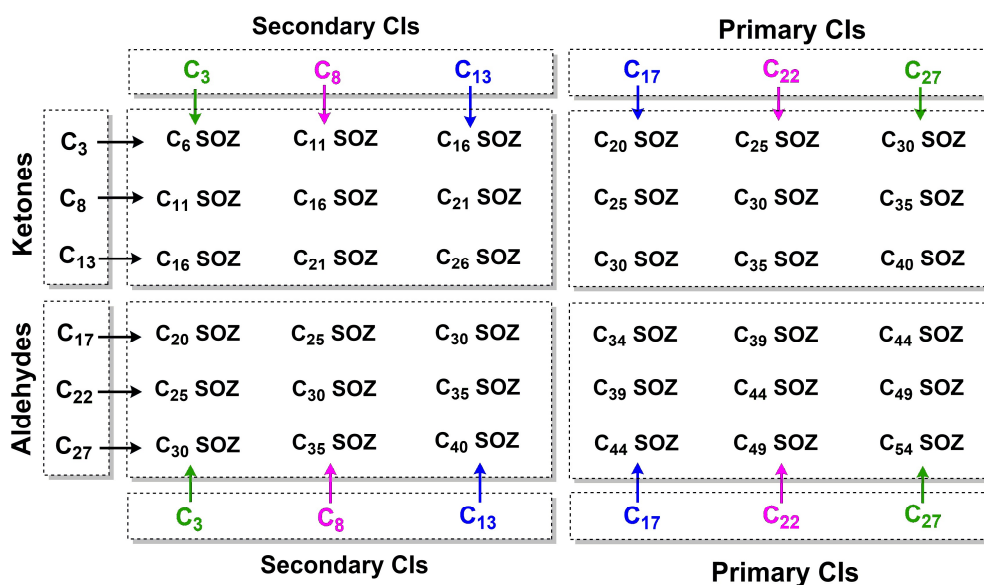
51 Section S2. Reaction mechanisms

52 This section presents supporting reaction mechanisms, including the ozonolysis reactions of Sqs (Figs. S8-S10), reactions
 53 between SOZs with amines (Figs. S11-S13), and reactions between C₁₇ aldehyde (or carboxylic acid) with ethylamine (Fig.
 54 S14).



55

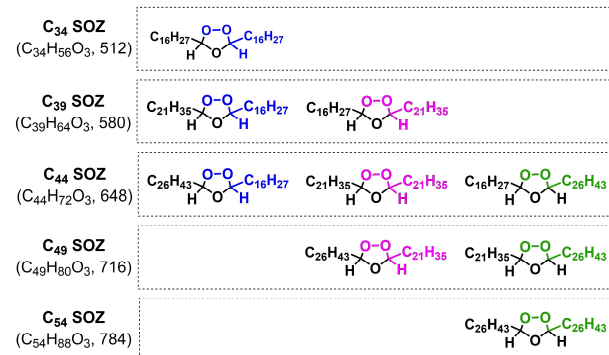
56 **Figure S8.** Ozonolysis of squalene (Sqe) yields aldehydes (*MW* 248, 316, and 384), ketones (*MW* 194, 126, and 58), and CIs. The
 57 isomerization reactions of primary CIs produce carboxylic acids (*MW* 264, 332, and 400).(Heine et al., 2017)



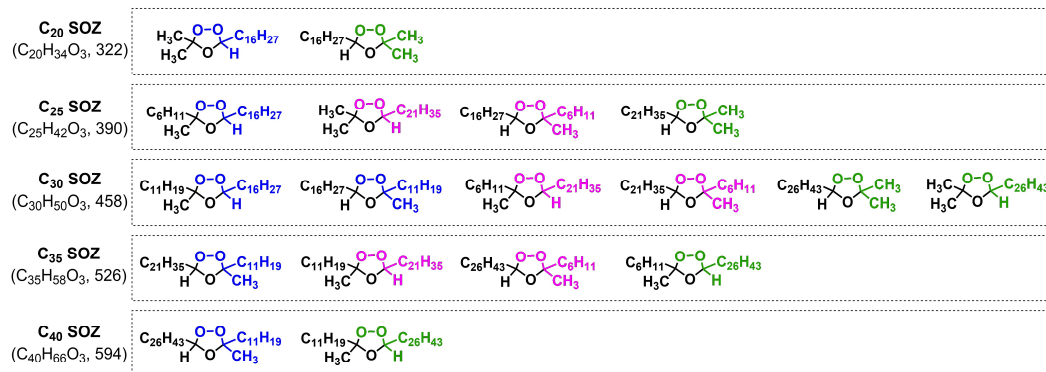
58

59 **Figure S9.** Bimolecular reactions between primary (or secondary) CIs and aldehydes (or ketones) leading to the formation of SOZs.

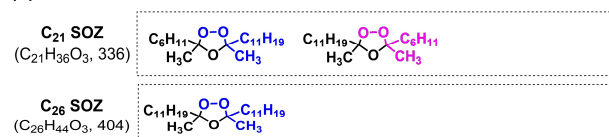
(a) disubstituted SOZs



(b) trisubstituted SOZs



(c) tetrasubstituted SOZs

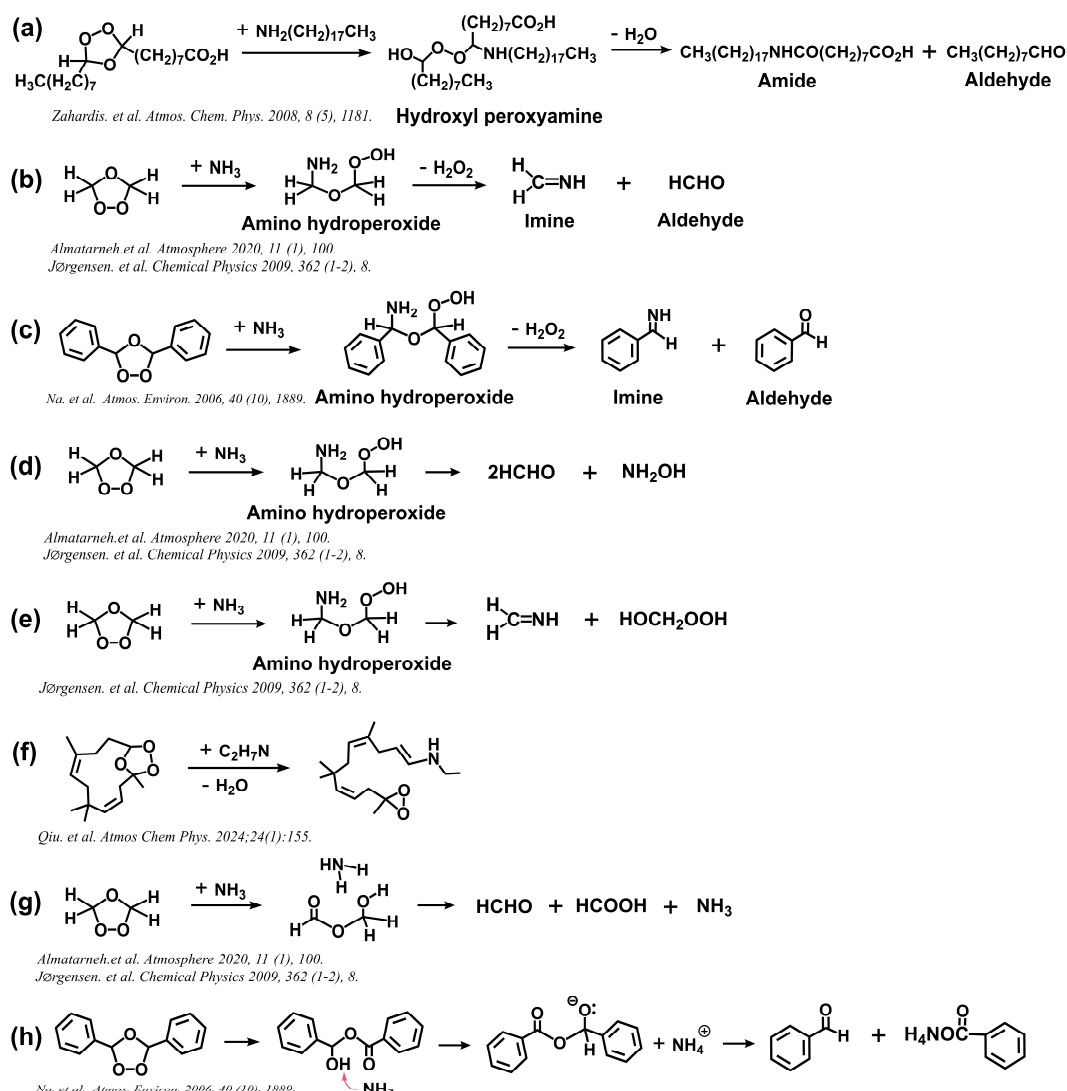


60

61 **Figure S10.** Structural classification of SOZs according to the number of alkyl substituents: (a) disubstituted (C₃₄, C₃₉, C₄₄, C₄₉ and C₅₄), (b)
62 trisubstituted (C₂₀, C₂₅, C₃₀, C₃₅ and C₄₀), and (c) tetrasubstituted (C₂₁ and C₂₆) SOZs.

63 Figure S11 illustrates established reaction mechanisms of SOZs with amines, highlighting mechanistic controversies (Qiu et
64 al., 2024; Zahardis et al., 2008; Almatrneh et al., 2020; Jørgensen and Gross, 2009; Na et al., 2006). Zahardis et al. (2008)
65 identified a reaction pathway of a C₁₈ SOZ with octadecylamine to generate a hydroxyl peroxyamine, which undergoes
66 dehydration to yield nonanal and a C₂₇ amide. In contrast, Almatrneh et al. (2020), Jørgensen and Gross (2009), and Na et al.
67 (2006) proposed the formation of amino hydroperoxides in SOZ + amine reactions (Almatrneh et al., 2020; Jørgensen and
68 Gross, 2009). Qiu et al. (2024) characterized a direct amination pathway where cyclic SOZ reacts with ethylamine via

69 concerted H₂O elimination, producing linear amination product (Fig. S11f). Additional pathways have been also proposed in
 70 Refs (Almatarneh et al., 2020; Jørgensen and Gross, 2009; Na et al., 2006) (Figs. S11g and S11h).



71
 72 **Figure S11.** Reaction mechanisms of SOZs with amines as established in previous studies (Qiu et al., 2024; Zahardis et al., 2008; Almatarneh
 73 et al., 2020; Jørgensen and Gross, 2009; Na et al., 2006).

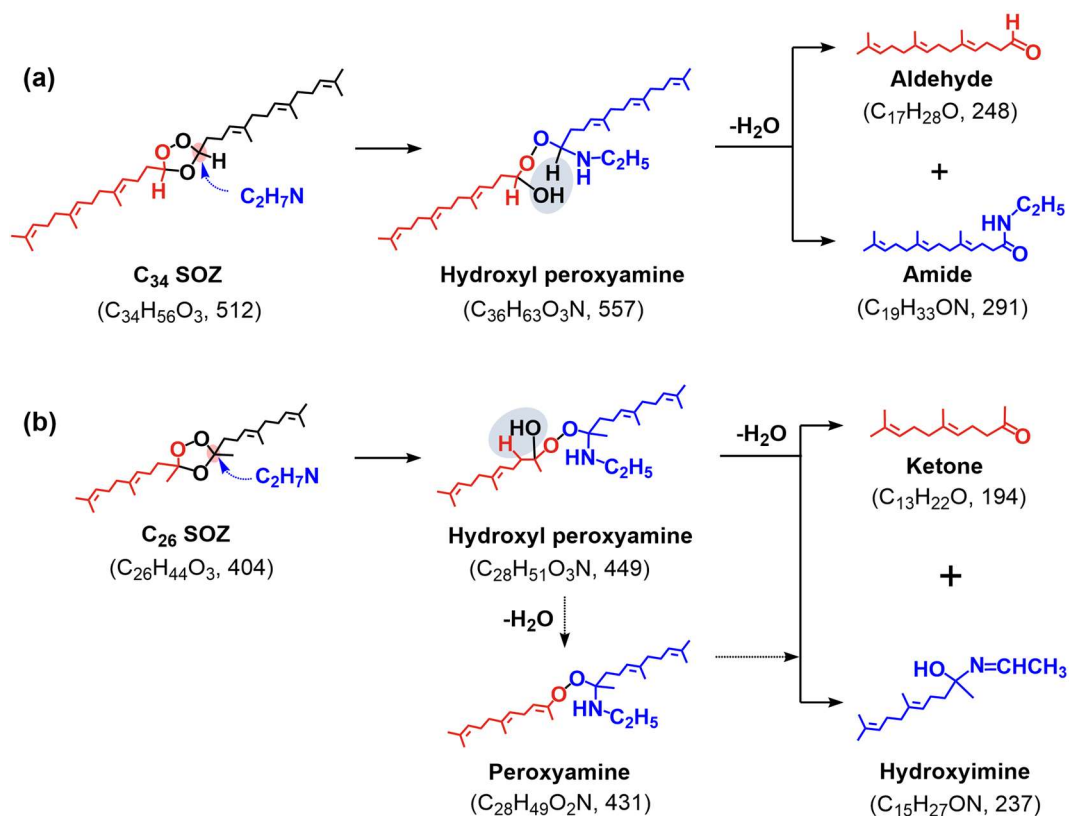
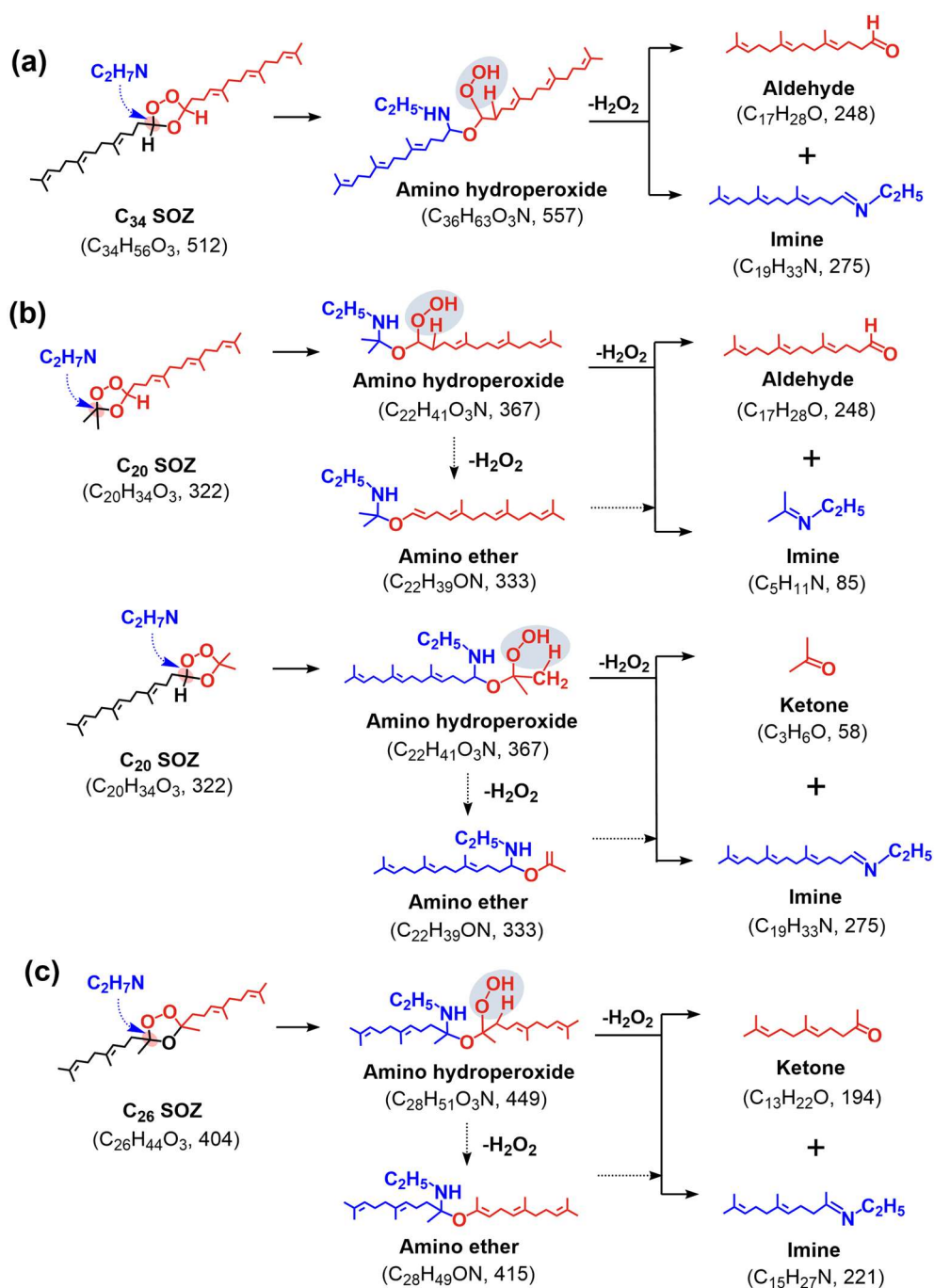
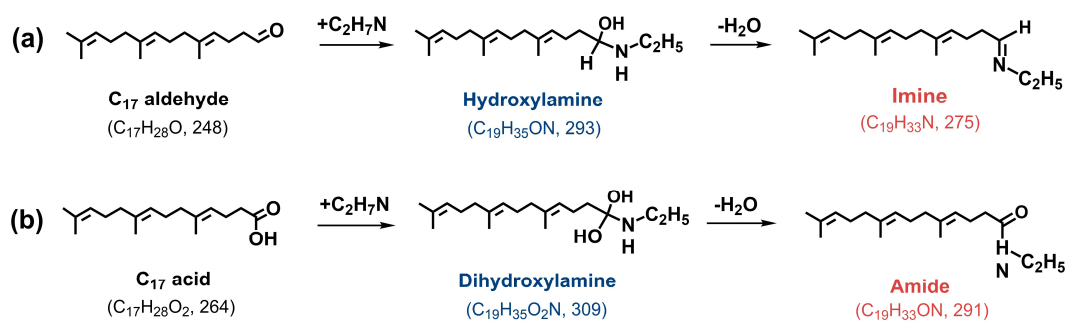


Figure S12. Reaction pathways of representative SOZs with varying alkyl substitution patterns: (a) disubstituted (C₃₄) and (b) tetrasubstituted (C₂₆) SOZs upon exposure to ethylamine (C₂H₇N).



77

78 **Figure S13.** Reaction pathways of representative SOZs with varying alkyl substitution patterns: (a) disubstituted (C₃₄), (b) trisubstituted
 79 (C₂₀), and (c) tetrasubstituted (C₂₆) SOZs upon exposure to ethylamine (C₂H₇N).



80

81 **Figure S14.** Reaction pathways of (a) C₁₇ aldehyde and (b) C₁₇ carboxylic acid upon ethylamine exposure.

82

83 **SI References**

- 84 Almatarneh, M. H., Alrebei, S. F., Altarawneh, M., Zhao, Y., and Abu-Saleh, A. A.-A.: Computational Study of the Dissociation
 85 Reactions of Secondary Ozonide, *Atmosphere.*, 11, 100-110, <https://doi.org/10.3390/atmos11010100>, 2020.
- 86 Heine, N., Houle, F. A., and Wilson, K. R.: Connecting the Elementary Reaction Pathways of Criegee Intermediates to the
 87 Chemical Erosion of Squalene Interfaces during Ozonolysis, *Environ. Sci. Technol.*, 51, 13740-13748,
 88 <https://doi.org/10.1021/acs.est.7b04197>, 2017.
- 89 Jørgensen, S. and Gross, A.: Theoretical investigation of reactions between ammonia and precursors from the ozonolysis of
 90 ethene, *Chem. Phys.*, 362, 8-15, <https://doi.org/10.1016/j.chemphys.2009.05.020>, 2009.
- 91 Liu, P., Gao, J., Xiao, X., Yuan, W., Zhou, Z., Qi, F., and Zeng, M.: Investigating the Kinetics of Heterogeneous Lipid
 92 Ozonolysis by an Online Photoionization High-Resolution Mass Spectrometry Technique, *Anal. Chem.*, 96, 19576-19584,
 93 <https://doi.org/10.1021/acs.analchem.4c04404>, 2024.
- 94 Na, K., Song, C., and Cockeriii, D.: Formation of secondary organic aerosol from the reaction of styrene with ozone in the
 95 presence and absence of ammonia and water, *Atmos. Environ.*, 40, 1889-1900, <https://doi.org/10.1016/j.atmosenv.2005.10.063>,
 96 2006.
- 97 Qiu, J., Shen, X., Chen, J., Li, G., and An, T.: A possible unaccounted source of nitrogen-containing compound formation in
 98 aerosols: amines reacting with secondary ozonides, *Atmos. Chem. Phys.*, 24, 155-166, [https://doi.org/10.5194/acp-24-155-](https://doi.org/10.5194/acp-24-155-2024)
 99 [2024](https://doi.org/10.5194/acp-24-155-2024), 2024.
- 100 Zahardis, J., Geddes, S., and Petrucci, G. A.: The ozonolysis of primary aliphatic amines in fine particles, *Atmos. Chem. Phys.*,
 101 8, 1181-1194, <https://doi.org/10.5194/acp-8-1181-2008>, 2008.